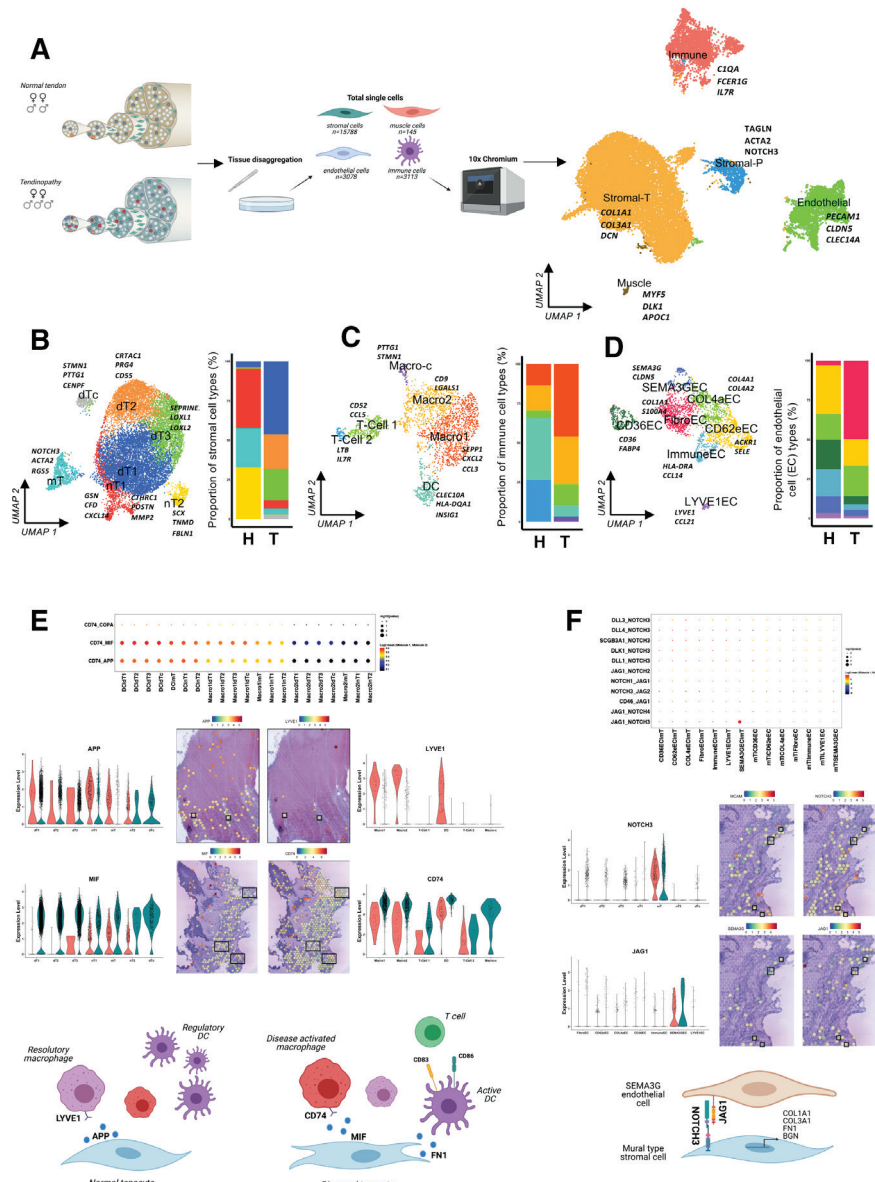


## Single cell and spatial transcriptomics in human tendon disease indicate dysregulated immune homeostasis

Tendinopathy; encompassing multifactorial tendon disorders characterised by pain and functional limitation remains a significant burden in musculoskeletal medicine.<sup>1</sup> Recent findings highlight a key role for immune mediated mechanisms in tendon disease supporting the concept that pivotal immunological and



**Figure 1** Cell composition and interactions of healthy and diseased human tendon. (A) Normal (n=4, human hamstring tendon) and diseased (tendinopathy, n=5, human supraspinatus tendon) human tendon were processed for single cell analysis using Chromium 10x 3' DEG chemistry. Infographic shows number of donors and cells sequenced. Uniform manifold approximation and projection (UMAP) embedding of 22124 single cells delineating endothelial, immune, stromal tenocyte and stromal mural cells with marker genes. (B) Stromal cells of the tendon. UMAP embedding with gene markers and distribution of seven delineated stromal cell populations from human tendons; mural tenocyte (mT), normal tenocyte1 (nT1), normal tenocyte2 (nT2), diseased tenocyte1 (dT1), diseased tenocyte2 (dT2), diseased tenocyte3 (dT3) and diseased cycling tenocytes (dTc). (C) Immune cells of the tendon. UMAP embedding with gene markers and distribution of 6 delineated immune cell populations from human tendons; dendritic cells (DC), macrophage1 (Macro1), macrophage1 (Macro2), cycling macrophage (Macro-C), T-Cells1 (T-Cell1) and T-Cells2 (T-Cell2). (D) Endothelial cells (EC) of the tendon. UMAP embedding with gene markers and distribution of seven delineated EC populations from human tendons; CD36 high EC (CD36EC), E-Selectin EC (CD62eEC), collagen 4 vessel EC (COL4aEC), immune-like EC (ImmuneEC), LYVE1 positive EC (LYVE1EC) and SEMA3G positive EC (SEMA3GEC). (E) Tenocyte-immune interactions in tendon (n=3 healthy vs 4 diseased). Predicted cell-cell interactions using CellphoneDB statistical framework on human tendon immune and stromal cells. Selected ligand receptor interactions showing APP and MIF ligand-receptor pairs in tendon stromal and immune cells. Mean of combined gene expression of interaction pairs (Log2 mean) and p value of specificity of interactions. Violin plots of APP and MIF expression in tendon stromal cells from healthy (pink) and diseased (green) tendon. Spatial expression (log2FC) of stromal APP and macrophage LYVE1 in normal human tendon and stromal MIF and macrophage CD74 in tendinopathic tendon visualised on 10x Genomics visium data, boxes highlight areas of coexpression. Violin plots of LYVE1 and CD74 expression in immune cells from healthy (pink) and diseased (green) tendon. Biorender infographic summarising tenocyte-immune cell interactions in tendon disease. (F) EC-tenocyte interactions in tendon. Predicted cell-cell interactions using CellphoneDB statistical framework on selected human tendon endothelial and stromal cells. Ligand-receptor interactions showing NOTCH3 ligand-receptor pairs in tendon endothelial and stromal cells. Mean of combined gene expression of interaction pairs (Log2 mean) and p value of specificity of interactions. Violin plots of NOTCH3 and JAG1 expression in tendon stromal and ECs, respectively from healthy (pink) and diseased (green) tendon. Spatial expression (log2FC) of NOTCH3 and MCAM from mural tenocytes and SEMA3G and JAG1 from SEMA3GEC's in human diseased tendon visualised on 10x Genomics visium data, boxes highlight areas of coexpression. Biorender graphic of predicted SEMA3GEC and mT interaction in human tendon.

biomechanical factors conventionally associated with inflammatory rheumatic and musculoskeletal diseases (RMDs) are manifest in tendon.<sup>2</sup> Single cell technologies<sup>3</sup> (scRNASeq) are increasingly applied in rheumatology to identify key cellular phenotypes that drive disease pathogenesis. Despite efforts with small cell numbers and heterogenous tendon biopsies<sup>4</sup> there remains no detailed spatial tendon cell atlas to inform translational targeting. Herein, for the first time utilising scRNASeq and spatial transcriptomics ( $S_T$ ), we carry out cell–cell interaction analysis to build an atlas of the dynamic cellular environment that drives the development of chronic human tendon disease.

In healthy (4 biopsies, n=3040 cells) and diseased (5 biopsies, n=19 084 cells) tendon we find a mix of endothelial, immune and stromal cells (figure 1A, online supplemental file 1). Each cell type group is present in disease and healthy tissue but with distinct quantitative and qualitative characteristics. Within stromal populations we identified ‘mural type’ stromal cells (figure 1B). Mural cells, which include pericytes, are possible progenitor cells in tendon<sup>5</sup> and interestingly, these cells are phenotypically similar to NOTCH3 high mural cells described in rheumatoid arthritis (RA) synovium which can differentiate into fibroblasts following interactions with endothelial cells (ECs) via JAG1.<sup>6</sup> Cell–cell interaction and  $S_T$  analysis indicate a similar phenomenon could occur within tendinopathy between mural cells and SEMA3G ECs (figure 1F). In all diseased stromal cell populations, there was greater expression of genes for extracellular matrix proteins (eg, COL1A1, COL3A1, FN1, BGN) which is considered the hallmark feature of tendinopathy (online supplemental figure S2B). Furthermore, pathway analysis indicates stromal cell clusters shift from negative regulation of immune cell and cytokine responses in normal tendon (online supplemental figure S3A) to a state that promotes immune cell recruitment and activation along with cytokine secretion and response processes in diseased tendon (online supplemental figure S3B,C).

Seven subtypes of PECAM1+ ECs were found (figure 1D), including a population of LYVE1+ ECs that produce CCL21 and have been shown to regulate dendritic cell (DC) migration.<sup>7</sup> Furthermore, CCL21 is upregulated in these cells in tendinopathy (online supplemental figure S2C). DCs comprise the single largest immune cell population present in normal tendon (figure 1B). Intriguingly, DCs are also present in diseased tendon however, showing therein greater levels of DC activation and lower levels of C1Q genes (regulatory DC markers) (online supplemental figure S2D,E). The activation of DCs and subsequent T cell activation<sup>8</sup> in tendinopathy is further evidenced by pathway analysis of differentially upregulated genes in disease (online supplemental figure S3D,E). This activation may in part be due to increased matrix protein expression, such as FN1, which can activate DCs and resulting in alterations in T cell populations within tissue potentially contributing to mechanisms driving disease chronicity. Additionally, we found three populations of macrophages in diseased tendon, one of which, cycling macrophages (figure 1C, online supplemental figure S2A) is unique to diseased tissue. The transcript profile of macrophages in normal tendon most closely resembled tissue repair and debris clearance (figure 1E, online supplemental figure S2D). Within normal tendon we found APP expression in tenocytes which can induce a resolution promoting phenotype in macrophages. However, APP expression was reduced in the stromal compartment in disease coinciding with diminished expression of LYVE1 within diseased tissue macrophages (figure 1E, online supplemental figure S2D). These macrophage subsets have recently been associated with RA remission and we postulate the

phenotypic drift away from this phenotype promotes aberrant tissue repair and attendant tendinopathy.<sup>9</sup>

Further evidence suggesting that the stromal environment may induce inflammatory changes comprises increased expression of MIF (figure 1E, online supplemental figure S2B) in diseased tenocytes that can induce proinflammatory effects via its receptor CD74, which is also upregulated in macrophages from diseased tendon (figure 1E, online supplemental figure S2C).  $S_T$  generated indicative data from cell–cell interaction analysis suggests stromal induced immune regulation. As such, we postulate the primary role of the immune compartment within the tendon is to regulate and resolve damage; however, following cumulative microtrauma the fundamental process of debris removal and matrix repair initiated by tenocytes could lead to positive amplification of the immune compartment. We further propose that within diseased tendon immune homoeostasis may become imbalanced and activated immune cells, primed by both endothelial and stromal cells, promote a cycle of inflammation and aberrant tissue repair. The inflammatory environment, including cytokine pathways that are unequivocally demonstrated in this preliminary tendon atlas, have been targeted to yield potent immunological interventions in a range of inflammatory RMDs—the potential to target and investigate these pathways in human tendon disease is now compelling.

**Moeed Akbar** , **Lucy MacDonald** , <sup>1,2</sup> **Lindsay A N Crowe**, <sup>1</sup> **Konstantin Carlberg** , <sup>3</sup> **Mariola Kurowska-Stolarska** , <sup>1,2</sup> **Patrik L Ståhl**, <sup>3</sup> **Sarah J B Snelling**, <sup>4</sup> **Iain B McInnes**, <sup>1,2</sup> **Neal L Millar** 

<sup>1</sup> Institute of Infection, Immunity and Inflammation, College of Medical Veterinary and Life Sciences, University of Glasgow, Glasgow, UK

<sup>2</sup> Research into Inflammatory Arthritis Centre Versus Arthritis (RACE), University of Glasgow, Glasgow, UK

<sup>3</sup> Science for Life Laboratory, Dept. of Gene Technology, KTH Royal Institute of Technology, Solna, Sweden

<sup>4</sup> Nuffield Department of Orthopaedics, Rheumatology and Musculoskeletal Sciences, University of Oxford, Oxford, UK

**Correspondence to** Mr Neal L Millar, Institute of Infection, Immunity and Inflammation, University of Glasgow, Glasgow G12 8TA, UK; [neal.millar@glasgow.ac.uk](mailto:neal.millar@glasgow.ac.uk)

**Handling editor** Josef S Smolen

**Twitter** Neal L Millar @tendonglasgow

**Acknowledgements** We thank the CZI Tendon Seed Network for helpful discussions when preparing this manuscript for publication.

**Contributors** MA, LM and NM conceived and designed the experiments. MA, LM and KC performed experiments. IBM, NM, LANC, PS and SJBS provided expert advice. All authors analysed the data. MA, LANC, IBM and NM wrote the paper.

**Funding** This work was funded by the Medical Research Council (MR/R020515/1). SJBS was funded by the NIHR Oxford Biomedical Research Centre.

**Competing interests** KC and PS are scientific consultants to 10x Genomics.

**Patient consent for publication** Not required.

**Ethics approval** All procedures and protocols were approved by the Ethics Committee under the approval number West of Scotland REC (REC14/WS/1035) with informed consent obtained and carried out in accordance with standard operative procedures.

**Provenance and peer review** Not commissioned; externally peer reviewed.

**Supplemental material** This content has been supplied by the author(s). It has not been vetted by BMJ Publishing Group Limited (BMJ) and may not have been peer-reviewed. Any opinions or recommendations discussed are solely those of the author(s) and are not endorsed by BMJ. BMJ disclaims all liability and responsibility arising from any reliance placed on the content. Where the content includes any translated material, BMJ does not warrant the accuracy and reliability of the translations (including but not limited to local regulations, clinical guidelines, terminology, drug names and drug dosages), and is not responsible for any error and/or omissions arising from translation and adaptation or otherwise.



## OPEN ACCESS

**Open access** This is an open access article distributed in accordance with the Creative Commons Attribution 4.0 Unported (CC BY 4.0) license, which permits others to copy, redistribute, remix, transform and build upon this work for any purpose, provided the original work is properly cited, a link to the licence is given, and indication of whether changes were made. See: <https://creativecommons.org/licenses/by/4.0/>.

© Author(s) (or their employer(s)) 2021. Re-use permitted under CC BY. Published by BMJ.

► Additional supplemental material is published online only. To view, please visit the journal online (<http://dx.doi.org/10.1136/annrheumdis-2021-220256>).



**To cite** Akbar M, MacDonald L, Crowe LAN, et al. *Ann Rheum Dis* 2021;80:1494–1497.

Received 1 March 2021

Accepted 5 May 2021

Published Online First 17 May 2021

*Ann Rheum Dis* 2021;80:1494–1497. doi:10.1136/annrheumdis-2021-220256

### ORCID iDs

Moeed Akbar <http://orcid.org/0000-0002-6923-4724>

Lucy MacDonald <http://orcid.org/0000-0001-7727-3873>

Konstantin Carlberg <http://orcid.org/0000-0002-1774-6058>

Mariola Kurowska-Stolarska <http://orcid.org/0000-0003-2124-7777>

Neal L Millar <http://orcid.org/0000-0001-9251-9907>

### REFERENCES

- 1 Millar NL, Silbernagel KG, Thorborg K, et al. Tendinopathy. *Nat Rev Dis Primers* 2021;7:1.
- 2 Gracey E, Burssens A, Cambré I, et al. Tendon and ligament mechanical loading in the pathogenesis of inflammatory arthritis. *Nat Rev Rheumatol* 2020;16:193–207.
- 3 Cheung P, Khatri P, Utz PJ, et al. Single-cell technologies - studying rheumatic diseases one cell at a time. *Nat Rev Rheumatol* 2019;15:340–54.
- 4 Kendal AR, Layton T, Al-Mossawi H, et al. Multi-Omic single cell analysis resolves novel stromal cell populations in healthy and diseased human tendon. *Sci Rep* 2020;10:13939.
- 5 De Micheli AJ, Swanson JB, Disser NP, et al. Single-Cell transcriptomic analysis identifies extensive heterogeneity in the cellular composition of mouse Achilles tendons. *Am J Physiol Cell Physiol* 2020;319:C885–94.
- 6 Wei K, Korsunsky I, Marshall JL, et al. Notch signalling drives synovial fibroblast identity and arthritis pathology. *Nature* 2020;582:259–64.
- 7 Murphy PM. Double duty for CCL21 in dendritic cell trafficking. *Immunity* 2010;32:590–2.
- 8 Garcia-Melchor E, Cafaro G, MacDonald L, et al. Novel self-amplificatory loop between T cells and tenocytes as a driver of chronicity in tendon disease. *Ann Rheum Dis* 2021;80:1075–85.
- 9 Alivernini S, MacDonald L, Elmesmari A, et al. Distinct synovial tissue macrophage subsets regulate inflammation and remission in rheumatoid arthritis. *Nat Med* 2020;26:1295–306.

## Methods

### Tissue collection and preparation

All procedures and protocols were approved by the NHS West of Scotland Ethics Committee (REC14/WS/1035) and informed consent was obtained from all patients according to standard procedures. Supraspinatus and tendon samples were collected from patients with rotator cuff tears undergoing shoulder surgery (Table S1). Standardised patient demographics were obtained preoperatively and included age, sex, duration of shoulder symptoms experienced by the patient and the number of subacromial steroid injections. Patients were only included if there was no clinically detectable evidence of subscapularis tendinopathy on a preoperative MRI scan as determined by a musculoskeletal radiologist or macroscopic damage to the subscapularis tendon at the time of arthroscopy as determined by the senior author (NLM)—by these criteria they represented a preclinical cohort. In this cohort, all patients fulfilled the following criteria: (1) a history of shoulder pain and dysfunction, (2) no previous surgery on the affected shoulder, (3) no radiographic sign of fracture of the shoulder and (4) no history of RA or osteoarthritis. Healthy (hamstring) tendon was obtained at the time of routine anterior cruciate ligament (ACL) reconstruction were employed as an independent control group. We acknowledge the limitation of utilising tendon from different anatomical sites. However, obtaining non-diseased shoulder tendon tissue from human subjects is extremely difficult and hamstring tendon has commonly been used in our own and other *in vitro* tendon studies as a surrogate control when comparing to diseased shoulder tendon.

### Single-cell RNA-seq

Single-cell suspensions of cells were derived from freshly digested tendon biopsies following surgical excision. Tendon tissue was digested in 0.15mg/ml Liberase TM (Sigma-Aldrich) in 10ml RPMI, kept in constant rotation at 37°C for a maximum of 2 hours. Digested tissue was then filtered and live cells were sorted using a FACS ARIA III. Isolated cells (13561 cells from healthy and 38040 cells from supraspinatus tendon tissue) were lysed and then RNA was reverse-transcribed and converted to cDNA libraries for RNA-seq analysis using a Chromium Controller and Chromium Single Cell 3' v2 Reagent kit (10x Genomics) following the manufacturer's protocol. Pooled libraries were used for sequencing on a HiSeq 4000 (Illumina) to a depth of ~30,000

reads per cell. Alignment of reads to the genome and generation of gene counts per cell were performed by Cell Ranger software (10x Genomics). 4080 cells from healthy and 22004 cells from supraspinatus tendon tissue were sequenced. Quality control was performed on each sample and poor-quality cells were removed on the basis of number of genes expressed (<200), of unique molecular identifiers (UMIs) and percentage of mitochondrial reads mapped (>5%). Following this QC, we normalised and scaled the data using Seurat v4.0 package (Sajita Lab) for all the cells (health k= 3040, supraspinatus k=19084). Then principal components analysis and high-quality cells were clustered using a graph-based routine implemented in Seurat R package and its integration method for multiple samples (Satija Lab). All cells from the tissue were clustered and individual cell types were computationally isolated for further analysis, including cluster markers and differential gene expression.

### **Cell-cell interactions**

Using the cluster markers found from Seurat we ran CellPhoneDB as follows:  
cellphonedb method statistical\_analysis meta.tsv counts.tsv—counts-data = gene\_name—threads = 60. CellPhoneDB raw predictions were filtered by removing those interactions with a  $P > 1.0 \times 10^{-5}$ . Significant pairs were then filtered for the most significant predicted interactions.

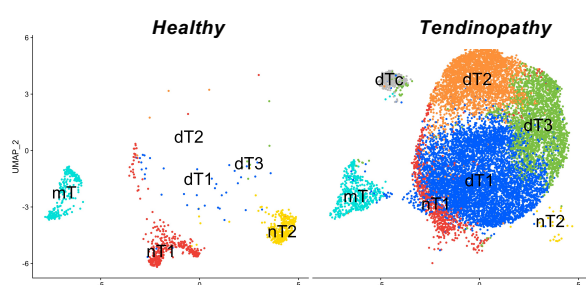
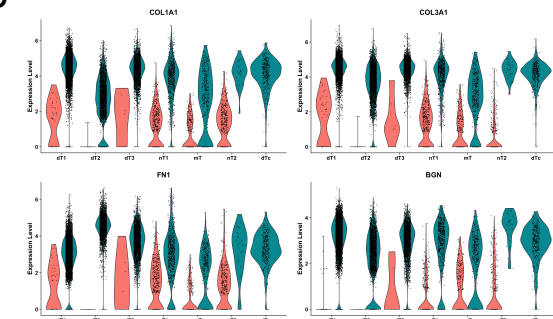
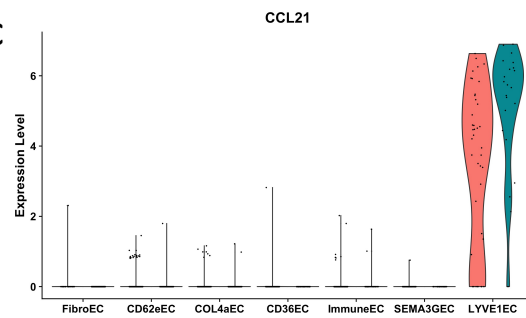
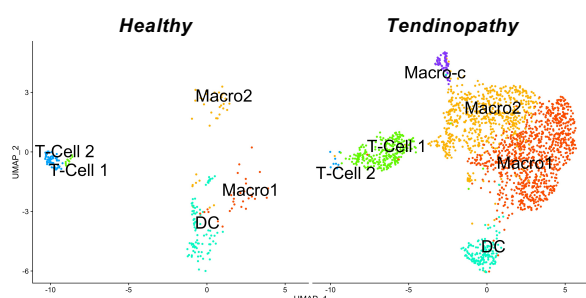
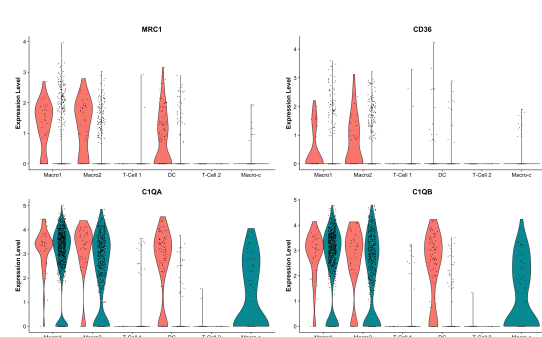
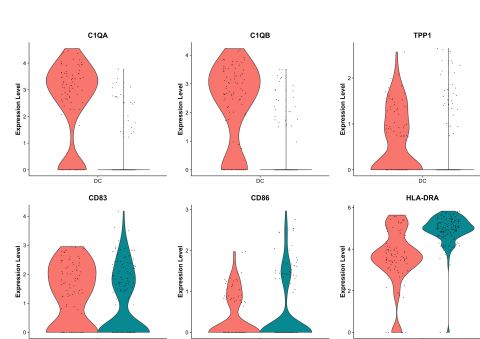
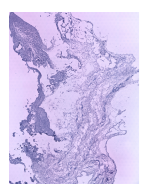
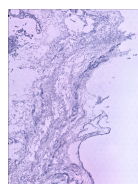
### Gene Ontology analysis

Gene ontology (GO) analysis was conducted by generating cluster markers and differentially expressed genes using Seurat as described above. The list of genes was then input into STRING (<https://string-db.org>) for functional enrichment analysis.

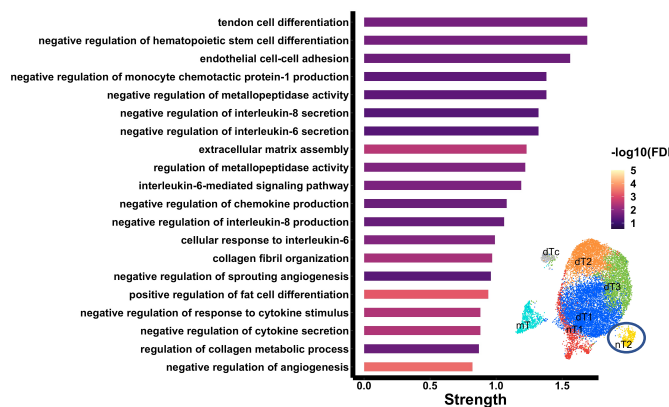
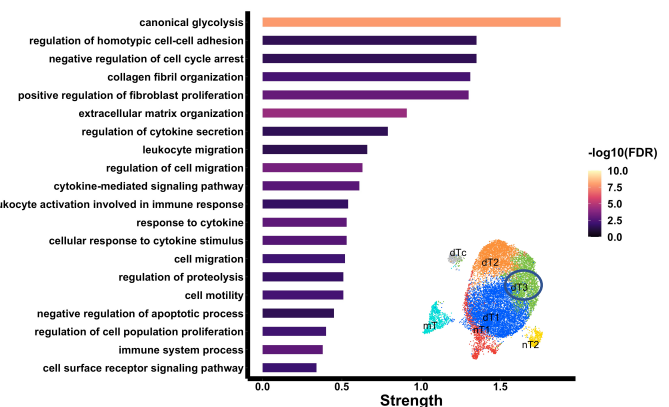
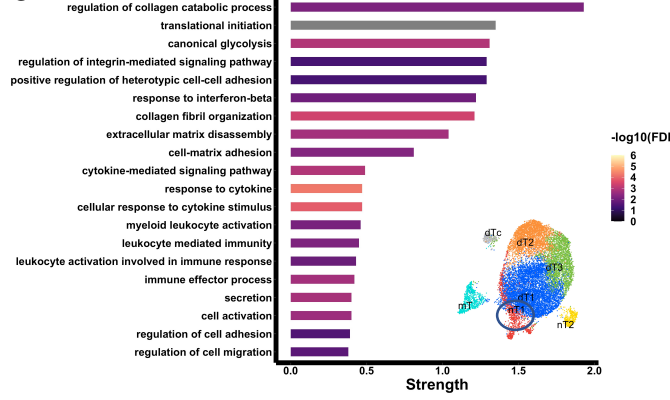
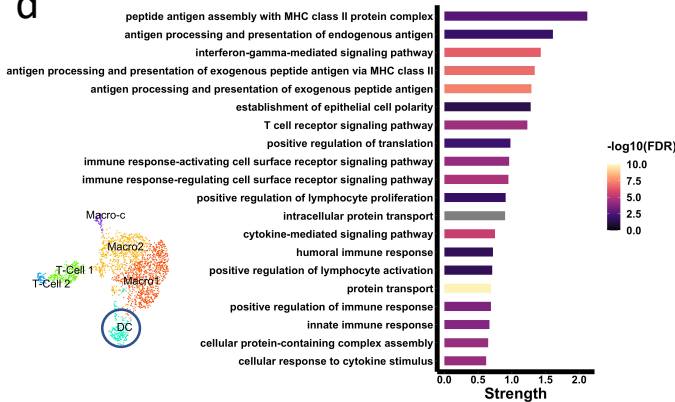
### **Spatial transcriptomics**

Visualisation of gene expression within tendon tissue was conducted using 10x Visium spatial gene expression kit(10x Genomics) as per manufacturers protocol on independent tendon tissue from samples used for single-cell RNA-seq. Briefly, additional healthy (n=3) and diseased tendon (n=4), collected as above, were immediately embedded in Optimal Cutting Compound (OCT) media and frozen in liquid-nitrogen-cooled isopentane bath, cut into 10 $\mu$ m sections using Thermo Scientific CryoStar cryostat, and mounted on 10X Visium slides, which were pre-cooled to -20°C. Slides were stained for H&E and then sections were imaged using Zeiss PALM

MicroBeam laser capture microdissection system and the images were stitched together using Zeiss software. The sections were then permeabilised for 10 minutes and spatially tagged cDNA library cDNA libraries constructed using the 10x Genomics Visium Spatial Gene Expression 3' Library Construction V1 Kit. cDNA libraries were sequenced on an Illumina NextSeq 500/550 using 150 cycle high output kits with sequencing depth of ~5000 reads per spot. Sequencing data and images were aligned using the Space Ranger 1.0.0 pipeline to derive a feature spot-barcode expression matrix (10X Genomics). Seurat 4.0 spatial expression workflow ([https://satijalab.org/seurat/articles/spatial\\_vignette.html](https://satijalab.org/seurat/articles/spatial_vignette.html)) was adopted to integrate, log-transform and normalised data before plotting genes of interest on section.

**a****b****c****Healthy****Tendinopathy****d****e****f****g****h**

Experiment	Tissue	Number of patients	Mean age in years (range)	Sex (M:F)
scRNASeq	Supraspinatus tendinopathy (established tendinopathy)	5	42.8 (33-55)	2:3
	Control tendon (hamstrings tendon)	4	32.8 (20-40)	2:2
S <sub>T</sub>	Supraspinatus tendinopathy (established tendinopathy)	4	48.8 (38-52)	2:2
	Control tendon (hamstrings tendon)	3	27.8 (21-30)	2:1

**a****b****c****d****e**